Chapter 7

Mould Fluxes in the Steel Continuous Casting Process

Elena Brandaleze, Gustavo Di Gresia, Leandro Santini, Alejandro Martín and Edgardo Benavidez

Additional information is available at the end of the chapter

http://dx.doi.org/10.5772/50874

1. Introduction

During the last decades, the continuous casting process has made enormous advances and more than 90% of the world steel production is now continuously cast [1]. In this process, the liquid steel is poured into a water-cooled copper mould through a submerged entry nozzle (SEN), see Figure 1 [2]. At this stage the solidification process begins. In this way semi-finished products with specific characteristics such as slabs and billets are obtained. During this process the mould fluxes perform several critical functions to obtain products with the quality required.

The mould fluxes are synthetic slags constituted by a complex mix of oxides, minerals and carbonaceous materials. The main oxides are silica (SiO_2), calcium oxide (CaO), sodium oxide (Na_2O), aluminum oxide (Al_2O_3) and magnesium oxide (MgO). The (CaO/SiO_2) ratios are 0.7 to 1.3 with fluorite (F_2Ca) and carbonaceous materials additions in their compositions. The compounds content ranges and their effects on mould fluxes behaviour at process conditions are summarized in Table 1.

These fluxes can be added through the top of the mould on the liquid steel, manually or automatically, the second way being the one that offers greater stability and constancy of the required properties.

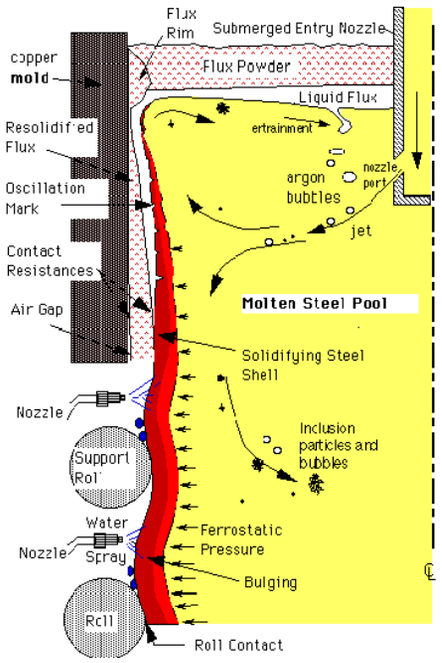

Figure 1. Schematic drawing of the continuous casting process [2].

Glass formers	SiO_2	17 – 56 %
	Al_2O_3	0 – 13 %
	B_2O_3	0 – 19 %
	Fe_2O_3	0 – 6 %
Basic oxides or modifiers	CaO	22 – 45 %
	MgO	0 – 10 %
	BaO	0 – 10 %
	SrO	0 – 5 %
Alkalis	Na_2O	0 – 25 %
	Li_2O	0 – 5 %
	K_2O	0 – 2 %
Fluidizing	F	2 – 15 %
	MnO	0 – 5 %
Melting control	C	2 – 20 %

Table 1. Typical composition of mould fluxes (wt %).

http://dx.doi.org/10.5772/50874

2. Mould fluxes functions

The continuous casting process is a very complex one which involves many variables: casting speed, mould oscillation characteristics, steel grade, mould dimensions and metal flow. All these variables need to be optimized but this is very difficult because it is not possible to see what is occurring inside the mould. In general, it is important to collect information on: analysis of plant data, simulations of different phenomena and measurements of different specific physical properties of the fluxes.

The additions of mould fluxes on the free liquid steel surface form different layers that are described in Figure 2. Each layer in isolation or combined with another one, provides the required functions of the powder.

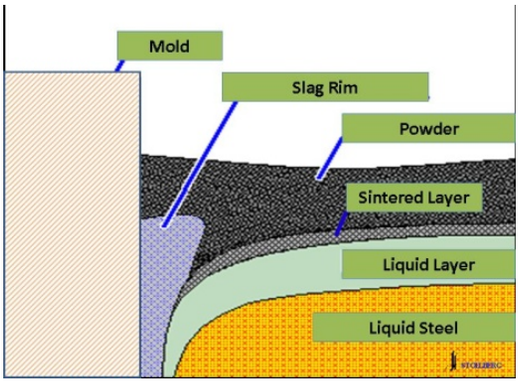

Figure 2. Different layers formed by the mould flux on the liquid steel.

The functions of the mould fluxes can be divided into two types, depending on the specific contact zone:

i) Zone of contact with the liquid steel

2.1. Thermal insulation

In this case, the objective is avoiding heat loss that could cause the premature solidification of the liquid steel in the meniscus zone. The properties of the mould fluxes that control these functions are:

- The mould flux density
- The thickness of the flux layer
- The carbon content
- The particle size distribution in the material

A bad thermal insulation in the meniscus promotes operation problems such as breakouts and could also cause surface defects in the products, such as cracks and oscillation deep marks.

2.2. Prevention of reoxidation

The liquid slag constitutes a barrier to avoid steel reoxidation by contact with air and the entrapment of other gases, such as nitrogen.

The steel reoxidation in the surface promotes oxide generation that could be incorporated as inclusions into the liquid steel (i.e. Al_2O_3) or into slag, changing its physical properties.

2.3. Inclusions entrapment

Mould fluxes are also designed to have the capacity to absorb or entrap inclusions in the interface of liquid slag–metal. In this way, it is possible to improve the cleanliness of the steel within certain operation parameters and depending on the process conditions. One of the important conditions is the depth of the liquid pool of slag [1].

The control of alumina (Al_2O_3) pickup in the liquid slag, during a certain period of time gives information of the slag absorption capacity. This oxide is produced by the reaction between the metal and the slag (Eq. 1):

$$4\ Al + 3\ SiO_{2\ (slag)} = 2\ Al_2O_3 + 3\ SiO_2 \quad (1)$$

The large particles can cross the slag/metal interface easily but the smaller inclusions need more time to do it. Absorption of inclusions can be enhanced using fluxes with high (CaO/SiO_2) ratios, high Na_2O, Li_2O and CaF_2 contents or low Al_2O_3, TiO_2 contents.

ii) Zone of contact with solidified steel

2.4. Lubrication between the solidified steel shell and the mould

Good lubrication is the most important function of the mould fluxes. The lubrication capacity of the liquid slag is related to the viscosity and the solidification temperature. For this reason, it is important to establish the viscosity values at operation temperatures by experimental tests or applying theoretical models. The lubrication is indirectly influenced by process conditions such as casting speed, superheat temperature and submerged nozzle (SEN) design. When the liquid slag layer is interrupted for any reason, sticker breakouts or cracks could occur. Surface cracks in slabs are also promoted by bad lubrication.

2.5. Heat transfer control

Heat transfer in the mould can be divided into horizontal and vertical heat transfer. The horizontal heat transfer has the more significant effect on the surface quality of the product. Nevertheless, the control of vertical heat flux permits to overcome problems such as pinholes and deep oscillation marks [1].

The heat transfer in the continuous casting mould is largely controlled by the film generated in the gap between the steel shell and the mould, due to the solid and liquid proportion characteristics of the slag. These characteristics are associated with the high or low crystallization tendency of the mould flux, because in this way a greater or lesser heat extraction can be controlled. For this reason, the mould flux has to be specifically selected for each steel grade.

http://dx.doi.org/10.5772/50874

3. Operation problems and product defects associated with mould fluxes

3.1. Sticking

Sticker breakouts occur when the solidified shell is broken in or out the mould and, as a consequence, the liquid steel can not be contained by the solidified shell. Figure 3 describes a normal shell formation and a distorted shell produced by a sticking.

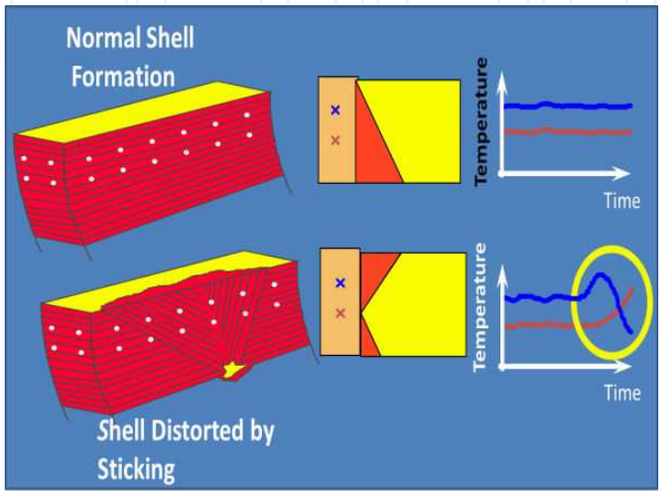

Figure 3. A normal steel shell formation and a distorted shell produced by sticking.

As it was mentioned, the mould fluxes are the responsible for providing a continuous lubrication between the mould and the strand This continuous lubrication has to be guaranteed because if it is interrupted, the steel sticks on the mould wall. This fact promotes considerable stresses due to the friction, increasing the risk of breakout.

In Figure 3, two solidification patterns are visualized: a normal solidification pattern and the solidification pattern when sticking occurs. In the right part of the figure, the graphics (temperature–time) show the behaviour of thermocouples during both mentioned situations.

The control system with thermocouples represents an important and effective tool in order to prevent damage of the steel shell by sticking. Another relevant application is to avoid the equipment detriment caused by the liquid steel leak. Possible causes of sticking problem to consider are:

a. Changes of the slag viscosity due to Al_2O_3 enrichment

b. Important variation of the liquid steel level

c. Oscillating system in poor conditions (change in the oscillation curve)

d. Interrupted lubrication by deficient mould flux supply

e. Freezing of the meniscus by poor insulation or by altering the flow pattern inside the mold.

3.2. Mould flux consumption

It is important to consider that the mould flux consumption gives information about the liquid slag infiltration between the mould and the steel shell, thus estimating the present lubrication. The consumption of mould powder depends on the process conditions and the materials characteristics. Shin et al. [3] reported results on the influence of the casting speed on mould powder consumption. Figure 4 show that when the casting speed increases, the mould powder consumption decreases.

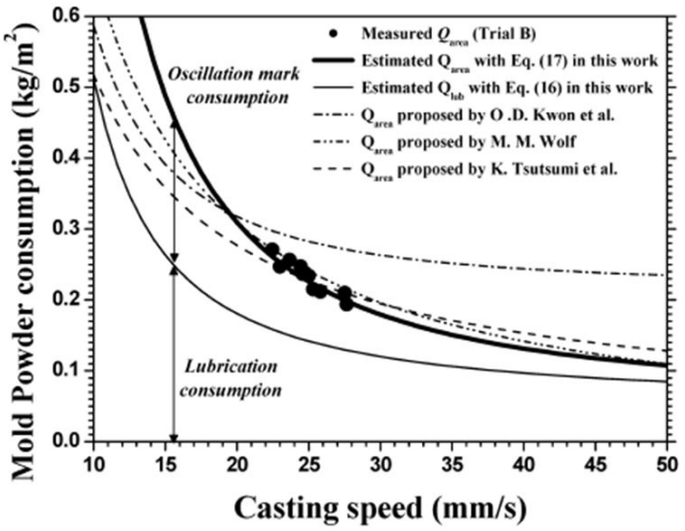

Figure 4. Influence of the casting speed on mould powder consumption [4].

Meng and Thomas [4] studied the influence of the mould oscillation parameters on the flux consumption. The authors concluded that oscillation frequency decrease implies lower powder consumption but higher oscillation amplitude or the increase in positive and negative strip increases the flux consumption.

3.3. Surface and subsurface defects

i) Slag entrapment

This type of defect may be associated with flow conditions and the physical properties of the liquid slag at steel meniscus level (see Figure 5). The main causes of this defect are associated with a high flow speed of the liquid steel at meniscus level. These conditions generate important forces that promote the entrapment of slag drops in the liquid steel. The viscosity and surface tension of the liquid slag constitute the primary physical properties related with the phenomenon of slag entrapment. Another reason for this type of entrapment be promoted, in the subsurface of the product, is the excessive changes of level in the mould. When the slag entrapments are large, they can interfere in the normal heat flow producing a thinner (and weaker) steel shell. As a consequence, the risk of breakout increases when the product leaves the mould.

http://dx.doi.org/10.5772/50874

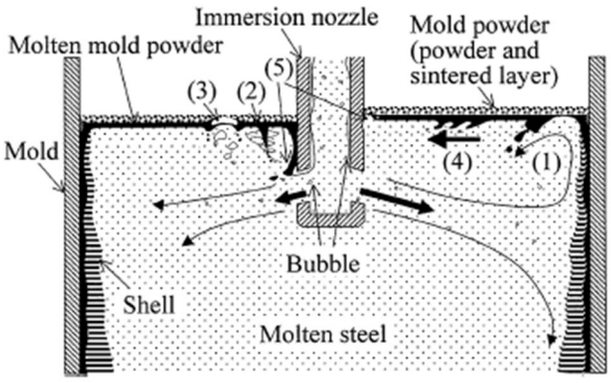

Figure 5. Mechanisms of slag entrapment indicated as 1, 2, 3, 4 and 5.

ii) Longitudinal crack

Steel grades with a chemical composition similar to peritectic steel are susceptible to develop longitudinal cracks. The origin of the problem involves the differences of the contraction coefficient between δ and γ iron that result in an irregular shell. As a consequence of stress concentration, the mentioned cracks are generated. Wolf [5] proposed the use of the carbon equivalent calculation in order to predict the longitudinal crack susceptibility. For example in the case of low alloy steel it is possible to use Eq.2 and Eq.3:

$$FP = 2.5 \cdot (0.5 - [\%C_P]) \tag{2}$$

$$\begin{aligned} Cp = {} & [\%C] + 0.04\,[\%\,Mn] + 0.10\,[\%\,Ni] + 0.70\,[\%\,N] - \\ & -0.14\,[\%\,Si] - 0.04\,[\%\,Cr] - 0.10\,[\%\,Mo] - 0.24\,[\%\,Ti] \end{aligned} \tag{3}$$

where FP is the ferrite potential and C_p is carbon equivalent for peritectic transformation. Here FP > 1 signifies a fully ferritic structure and FP < 0 means fully austenitic structure. This leads to classify the steel grades in two groups: type A with high depression tendency and type B with tendency to sticking and solidification cracking. FP criterion also predicts inner crack sensitivity.

The strategy to avoid the longitudinal crack is to obtain a homogeneous shell through a uniform heat extraction. The mould powder is the tool which permits to minimize the crack tendency and these tendencies decrease at higher powder consumption because the film thickness increases. All longitudinal cracks are formed near the meniscus zone.

4. Physicochemical properties and structure of mould fluxes

The knowledge of physicochemical properties of mould powders is necessary to solve problems in industry and to develop mathematical models of the process. Generally, the determination of these properties is very complex due to the high temperatures involved (usually higher than 1000°C) and the reactions with the containers of mould powders. Besides, it is necessary to know a large number of properties such as density, thermal conductivity, viscosity, melting temperatures, surface tension, etc. Due to the complexities of these measurements, mathematical models are often used. Since, the chemical composition is information available through the suppliers; this information is used to estimate the values of physicochemical properties at high temperature.

In order to estimate these properties more complex models that make use of the structure of the molten mould powders, phase equilibrium diagrams, thermodynamic data, and neural network based models, have been used. In all cases, it should be noted that the model results are compared to experimental data, which in turn, possess a certain degree of error. Accordingly, the accuracy of the results obtained by means of the models can not be greater than those obtained experimentally.

To compute the properties of the mould fluxes several models have been used. They can be classified in [6]: (i) numerical adjustments, (ii) neural networks, (iii) structure based models and (iv) thermodynamic models.

The structure of the mould fluxes is based on silicate chains of the silicon oxide (SiO_2), where each Si^{4+} ion is surrounded by four O^{2-} (tetrahedral structure SiO_4^{4-}). Each of the anion O^{2-} is connected to two others O^{2-} (called bridging oxygen) forming a three dimensional network. This network is broken when entering the cations type Na^+ or Ca^{2+}. These cations break silicate chains forming non-bridging oxygens O^- and free oxygens O^{2-} that are not bound to cations Si^{4+} but to the network breakers: Na^+, Ca^{2+}, Mg^{2+}, etc. [7].

Cations of type Al^{3+} can enter the polymer chain but they should be located close to others cations such Na^+ (or Ca^{2+}) to maintain the local charge balance. Cations Fe^{3+}, in low concentrations, act as network modifiers, while in greater proportions, may be incorporated into the chain silicate similarly to Al^{3+}.

Thus, the properties of the mould powders are affected by the composition and arrangement of the individual compounds. Namely, they depend on the concentration of network formers (SiO_2, Al_2O_3) and network modifiers (Na_2O, Li_2O, CaO, MgO, K_2O).

4.1. Viscosity

The viscosity (η) expresses the difficulty with which a layer of liquid moves over another. Thus, when the length of the chains Si-O increases, this difficulty also increases. Therefore, a higher viscosity is associated with a higher degree of polymerization (higher content of network formers).

http://dx.doi.org/10.5772/50874

On the one hand, mould powders called "glassy", present a smooth change in viscosity versus the temperature curve when during cooling the material changes from liquid to supercooled liquid at the glass transition temperature (T_g). This temperature is associated to a viscosity of $10^{13,4}$ Pa (Figure 6a). On the other hand, for mould powders called “crystalline” the curve logη vs 1/T presents a significant change in slope at the temperature at which crystallization begins (Figure 6b). This temperature is called "break temperature" (T_{br}).

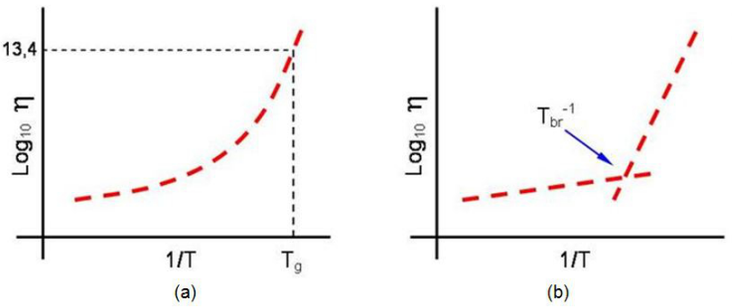

Figure 6. Plots of logη vs. 1/T of (a) glassy and (b) crystalline mould fluxes.

The viscosity of the molten material presents a significant dependence on temperature. This dependence is expressed by an equation of type Arrhenius (Eq. 4):

$$\eta = A_A.\exp(-E_A / R.T) \tag{4}$$

Or type Weymann (Eq. 5):

$$\eta = A_W.\exp(-E_W / R.T) \tag{5}$$

Where A_A, A_W are constants, R is the gas constant, and E_A, E_W are the activation energies for viscous flow.

Viscosity models of mould powders have been developed on a large amount of experimental data. A review of models based on the chemical composition [8] showed that the minor differences between the estimated values and those determined experimentally were presented by both the Iida and Riboud models. The greatest differences were within 30%.

The Riboud model [9] uses the following expression to compute the viscosity (Eq. 6):

$$\eta = A.T.\exp\left(\frac{B}{T}\right) \tag{6}$$

where T is temperature in Kelvin, and A and B are parameters obtained by means of the mould powder composition. On the other hand, in the Iida model [10] the expression for calculating the viscosity is (Eq. 7):

$$\eta = A.\eta_0 \exp\left(\frac{E}{B_i}\right) \tag{7}$$

where A and E are parameters set by adjustments to experimental data, η_o is the viscosity of the melted components not forming network and Bi is the modified basicity index.

An alternative method to compute the viscosity of mould fluxes was used by Brandaleze et al. [11]. This method is based on the model presented by Moynihan [12] that uses the width of the glass transition, which can be determined by DTA or DSC. According to this model, the viscosity can be calculated using the following equation (Eq. 8):

$$\log\eta = -5 + \frac{14.2}{[0.147(T - T'g)/(T'g)^2 \Delta(1/Tg)] + 1} \tag{8}$$

where η is the viscosity in Pa.s, T is the temperature in K, T_g is the glass transition temperature, T'_g is the end point of the glass transition and $\Delta(1/T'_g) = 1/T_g - 1/T'_g$.

Using Eq.8 the viscosity of two mould powders (10F and PC) between 1200-1450°C was estimated (Figure 7). Powder PC is of commercial origin and 10F was prepared in laboratory, both containing fluorine (for chemical composition see Table 2).

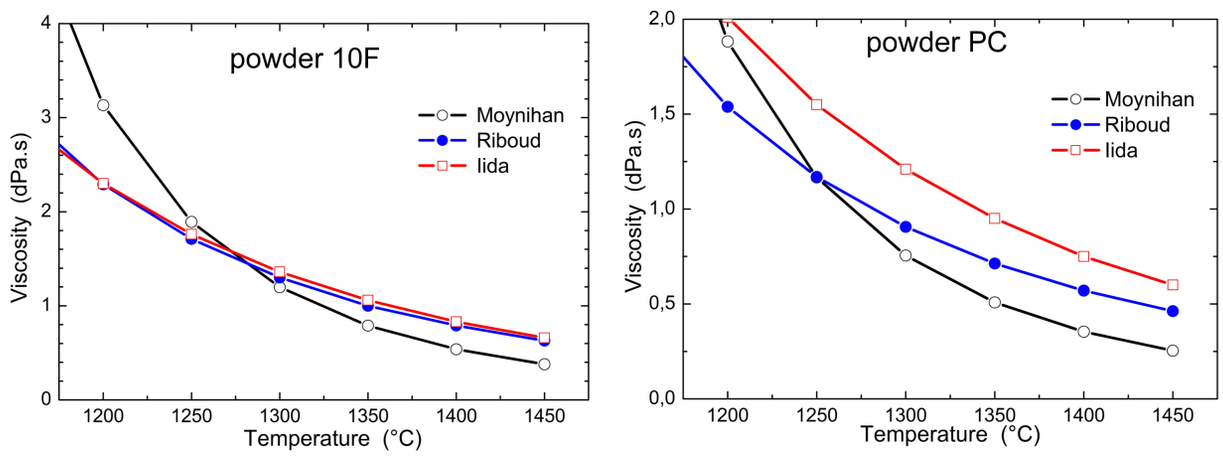

Figure 7. Viscosity values estimated from different methods.

The η-values calculated by this method were compared with those calculated for the Iida and Riboud models. The differences between the values of viscosity obtained by the Moynihan model with respect to these two traditional models were within 33%.

4.2. Thermal conductivity

The thermal conductivity of the liquid slag tends to increase as the SiO_2 content increases. This behaviour can be attributed to a better thermal conduction along the polymer chains. This transport is hindered by the presence of non-bridging oxygen (O^-) and cation breakers

http://dx.doi.org/10.5772/50874

at the ends of the polymer chains. This interpretation has been experimentally supported by Eriksson et al. [13] in a work on liquid slags in the system $CaO\text{-}Al_2O_3\text{-}SiO_2$.

On the other hand the thermal conductivity seems to be affected by the nature of the cations modifiers, according to the following relationship $k_{LiO2} > k_{Na2O} > k_{K2O}$ [14].

Thus, when the content of network formers increases, the higher is the thermal conductivity. Therefore, an increase in the thermal conductivity may be associated with an increase of the viscosity [14]. However, this behaviour is interpreted based on the heat conduction on the network (lattice) k_L, but contributions of the heat transfer by convection (k_C) in the liquid layer and radiation (k_R) are unknown.

When the melted mould flux layer solidifies, forming either crystalline or amorphous structures, it should be noted that heat transfer by radiation in a crystalline solid decreases due to scattering of radiation by the crystal, grain boundaries and pores. Thus, an amorphous solid (glass) has greater heat conduction by radiation than a crystalline one. When comparing a glassy mould flux with a crystalline one, below the onset of crystallisation temperature (T_{br}) the conduction by radiation will be lower in the crystalline solid.

The low reliability in measurements of thermal conductivity impacts in obtaining a reliable database to develop a secure model to estimate k based on temperature and chemical composition.

Furthermore, it should be noted that, during the continuous casting process, the first layer of slag that forms against the copper mould is glassy (because of high cooling rate). But then with time, it tends to crystallize. When this layer crystallizes, it contracts (high density) and generates pores, near the crystals, and a rough surface at the interface mould/slag which is equivalent to an air gap in this interface. This air gap is represented by an interfacial resistance $R_{Cu/sl}$. For example, Hanao and Kawamoto [15] calculated an interfacial resistance $R_{Cu/sl} = 0.2\ 10^{-3}\ m^2.W^{-1}.K^{-1}$, while Brandaleze et al. [16] measured $R_{Cu/sl} = 1.9 \times 10^{-3}\ m^2.W^{-1}.K^{-1}$. Thus, if the crystallization occurs with the time, this leads to a reduced flow of heat from the steel to the copper mould.

The relationship among k_R and k_L with the degree of crystallization was studied by Ozawa et al. [17]. They observed that: (i) k_L tends to increase with the degree of crystallization and (ii) k_R decreases until reaching a constant value when the fraction of crystals exceeds 15%. Meanwhile, Nakada et al. [18] studied the heat transfer through a mould flux layer and concluded that the k_R constitutes less than 20% of the total heat flow. The authors noted that the extraction of heat was very sensitive to both the thickness and the emissivity of the mould flux layer. So, if two mould powders that do not tend to crystallize on cooling (glassy) are compared, the one presenting a higher viscosity tends to generate a thicker layer of molten powder. This results in a lower extraction of heat in the hottest zone (top) of the mould.

4.3. Surface tension

This property is affected primarily by constituents who have the lowest values of surface tension (surfactants), which tend to occupy the surface layer of the liquid. The surface concentration depends on the surface tension (γ) and the activity of the components.

To estimate the surface tension different models have been used, being the simplest method that which uses partial molar fractions (X_i) of components [19]. In this model the components are divided into two classes: (i) oxides with high surface tension and (ii) components of lower surface tension or surfactants (such as B_2O_3, CaF_2, Na_2O, K_2O, Fe_2O_3) according to Eq. 9.

$$\gamma = X_1.\gamma_1 + X_2.\gamma_2 + X_3.\gamma_3 + ... \tag{9}$$

The uncertainties of this model are within ± 10%.

Another model [20] also used the molar volume of components and the ionic radii.

4.4. Liquidus and break temperatures

The liquidus temperature (T_{liq}) can be determined by DTA or DSC tests (melting endotherm) or by Hot Stage Microscopy (HSM). In the latter case T_{liq} must be associated to fluidity temperature (T_F). Due to the different components of these materials, the first occurrence of liquid is detected at a temperature lower to melt flow (T_F). The fluidity temperature is considered as one in which the material reaches a viscosity apt to flow into the mould-steel gap. Models to calculate T_{liq} based on chemical composition have a high degree of uncertainty.

Moreover, the break or crystallisation temperature (T_{br}) is usually between 1100-1200 °C. A numerical model to calculate T_{br} (within an error of ± 30°C) has been used [21]. These method estimates break temperature according to the following equation (Eq.10):

$$\begin{aligned} T_{br}(K) = 1393 - 8.4\%Al_2O_3 - 3.3\%SiO_2 + 8.65\%CaO - 13.86\%MgO - 18.4\%Fe_2O_3 \\ - 3.2\%MnO - 9.2\%TiO_2 - 2.2\%K_2O - 3.2\%Na_2O - 6.47\%F \end{aligned} \tag{10}$$

4.5. Melting rate

Although the melting rate depends on process parameters such as casting speed, it is also influenced by the quality and content of free carbon [22]. The melting rate decreases with increasing carbon content and/or its particle size decreases, and increases when the reactivity of the carbonaceous material is larger [23]. An estimation of the reactivity of the carbonaceous material can be performed if decomposition kinetics is known.

Benavidez et al. [24] conducted a study on the kinetics of decomposition of two carbonaceous materials: petroleum coke (sample C) and synthetic graphite (sample G). Both materials are often used to include free carbon in mould powders composition.

http://dx.doi.org/10.5772/50874

The activation energy (Ea) associated with the decomposition of carbonaceous materials was calculated using four methods applied to non-isothermal thermogravimetric curves (TG) performed at different heating rates. An average value of Ea ≈ 48 kJ/mol for the powder with 15 wt% of coke, and Ea ≈ 67 kJ/mol for the powder with 15 wt% of graphite was obtained from the different methods. The lower activation energy of the decomposition process of the coke is associated with increased reactivity of this carbonaceous material relative to the graphite. This behaviour is in agreement with the higher degree of crystallinity observed in the synthetic graphite, since the greater amount of crystals results in the need of a greater amount of energy (heat) to decompose the carbonaceous material (low reactivity).

4.6. Density and molar heat capacity

Because of the strong covalent type bonds that presents SiO_2, its coefficient of linear thermal expansion (α) is very low. Thus, as the value of α is proportional to the change of density with temperature ($d\varrho / dT$), then the density is slightly affected by the temperature. According to this, the value of α increases when the percentage of cations network modifiers increases. It is also observed that the coefficient of thermal expansion increases to a greater extent for M_2O monovalent oxides than for MO bivalent ones. In both cases, the coefficient of thermal expansion increases according to the following cation size relationship: K > Na > Li (oxides M_2O) and Ba > Ca > Mg (oxides MO). The density of the slags can be estimated using thermodynamic models [25]. However, considering the density of the liquid slag only slightly dependent on the structure, then one can use a simpler model to calculate its density in the liquid state. In this case molar volume (V) and molecular weight (M) of the mould powder are computed through Eq. 11:

$$\rho = \frac{M}{V} = \frac{\sum_i X_i.M_i}{\sum_i X_i.V_i} \tag{11}$$

where X_i is the mole fraction, M_i is the molecular weight and V_i is the molar volume of component i.

The molar heat capacity is not affected by the structure, but rather by the composition. Thus, a good estimation of mould flux (Cp) can be obtained from the mole fraction (X_i) and the heat capacity (Cp_i) of each component (Eq.12):

$$Cp = \sum_i X_i.Cp_i \tag{12}$$

If the mould powder is glassy, the value of Cp drops abruptly at glass transition temperature.

5. Experimental equipments and techniques to characterize mould powders

Experimental techniques are very important to characterize or previously evaluate the behaviour of a mould powder during the continuous casting process. The most important techniques are those that provide information about properties such as:

- Heat transfer
- Melting rate
- Viscosity / fluidity
- Critical temperatures

5.1. Heat transfer

Several operating problems and surface quality defects, which occur in the continuous casting process, are determined by the heat transfer through the flux layers. For this reason, it is important to perform measurements of thermal conductivity and compare the behaviours of the various types of fluxes used in the mould.

Many researchers have developed different experiments to measure thermal properties in melted fluxes trying to represent process conditions. Regardless of the measurement method used, the calculations are mainly based on the heat conduction laws (Eq. 13-15), allowing to determine the heat flow (q) [W/m^2], interfacial resistances (R) [m^2 K/W] and thermal conductivity of gap (k_{gap}) [W/m K]. In Eq. 13, k is the thermal conductivity of reference material and d the distance between the temperature measurement points.

$$q = k \cdot \frac{(\Delta T)}{d} \tag{13}$$

$$R = \frac{\Delta T}{q} \tag{14}$$

$$k_{gap} = \frac{q \cdot d_{gap}}{\Delta T} \tag{15}$$

The main methods and devices reported in the literature are described below.

Schwerdtfeger et al. [26] simulated the gap between the steel and the copper mould, moving a cooled copper block to a surface of molten flux on a steel plate heated by electrical resistance. The temperature was registered by three thermocouples (two in the copper mould and one in the steel), which are used to calculate the effective thermal conductivity (k_{gap}) and the radiation and conduction components.

http://dx.doi.org/10.5772/50874

Mikrovas et al. [27] and Jenkins et al. [28] used the "finger test" based on the immersion of a copper cylinder in a molten flux bath. The cylinder is fitted with thermocouples placed strategically from which it is possible to calculate the heat flow and thermal conductivity of the system.

Yamauchi et al. [29] measured the thermal resistance of the powder through the device of Figure 8a which used an AlN plate as hot side and a steel block as refrigerated cold side with the ability to regulate the thickness of mould powder located between them.

The laser pulse method was employed by Mills et al. [30] to measure the thermal conductivity on solidified flux samples. The value is obtained from the estimation of the thermal diffusivity, density and specific heat capacity.

Similarly to [26, 29] in the device built by Holzhauser et al. [31] the sample is placed on a steel plate. The cold zone is provided by a cooled copper block with thermocouples located at strategic points to determine the thermal conductivity. The system is heated by means of electrical current (Figure 8b).

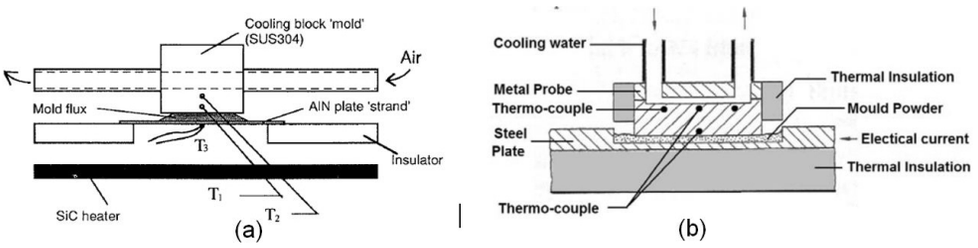

Figure 8. Experimental apparatus used to measure heat transfer through mould powder layers: (a) Yamauchi et al., and (b) Holzhauser et al.

Stone and Thomas [32] developed an equipment to simulate the mould conditions, based in a copper block and a steel plate to simulate the gap between mould and steel shell. The heat is applied on the steel plate by a torch. The molten powder is poured between the two plates. The different thermocouples placed in the equipment according to Figure 9 allow to calculate the thermal conductivity of molten flux using the equations 13 to 15.

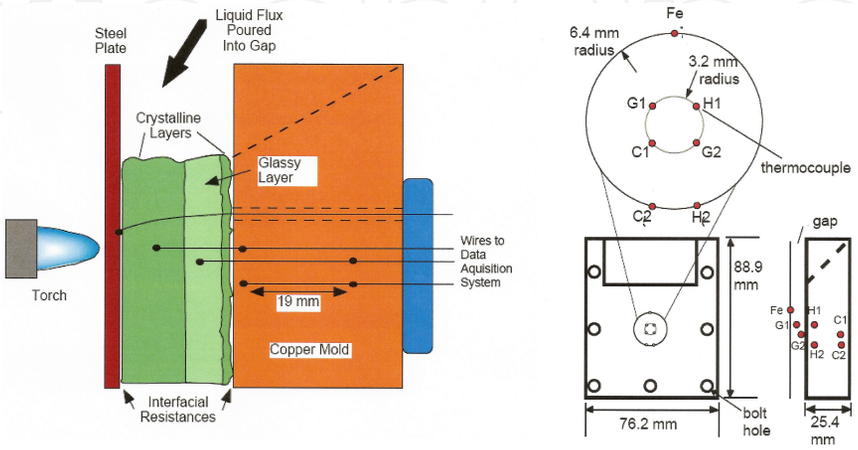

Figure 9. Heat transfer equipment developed by Stone and Thomas [32].

Brandaleze et al. [16] based on the Stone and Thomas design, made changes in both the positions of thermocouples and the cooling system, obtaining results in agreement with literature (Figure 10). Using this device Martin et al. [33] presented a comparison between a mould flux layer taken from a continuous casting machine, with another flux layer extracted from the heat transfer equipment. From the structural and microstructural analysis could be inferred that the thermal conductivity measurement is carried out under thermal conditions similar to those in the continuous casting process.

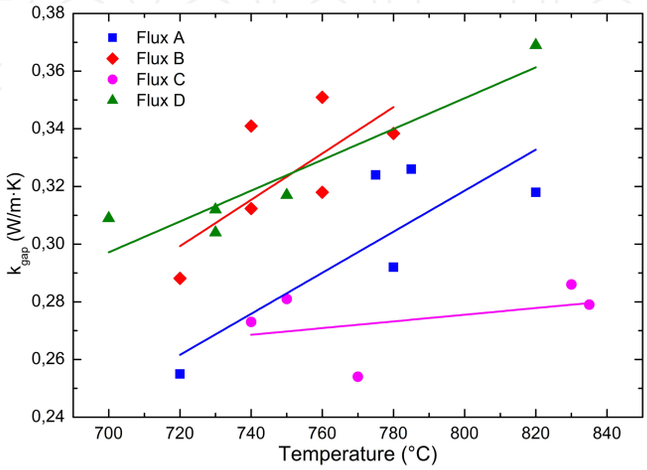

Figure 10. Heat transfer of four commercial mould powders.

5.2. Melting rate

The melting rate is an important property of the powder because it affects both the powder consumption and the depth liquid pool modifying the lubrication and heat transfer conditions. The main factor governing this property is the free carbon content. The C particles are not wetted by the molten flux and consequently separate the mineral particles delaying the agglomeration of the molten flux globules. For this reason, a higher content of free C promotes more time of agglomeration resulting in a lower melting rate.

There are basically two methods to measure this property:

i) Combustion capsules test

In this test 1.5 g of mould powder is placed in combustion capsules (porcelain) with one extreme closed and another open for easy viewing of the sample. Then, the capsule is heated inside a furnace and is observed through a horizontal window disposed for this purpose. The time taken to melt the sample is recorded and the melting rate is calculated. In this test the heat flow is unidirectional.

ii) Drip test

In this test the sample is placed in the conical base of a crucible and then molten mould flux drips out of the furnace. This molten flux is collected and weighted continuously by a balance placed at the bottom of the furnace.

http://dx.doi.org/10.5772/50874

5.3. Viscosity / Fluidity

As it was noted above the viscosity of mould flux has a decisive influence on the infiltration of liquid slag in the mould gap, which is probably the most important process in continuous casting because it affects the lubrication between the steel and the mould. The viscosity is also an important factor in the erosion of the refractory nozzle being a function of $1/\eta$.

High viscosity fluxes are frequently used to minimize slag entrapment. But in this case, the pressure developed by the molten slag in the mould-steel gap is high and can influence on the depth of the oscillation marks.

Several methods are used to measure the viscosity of mould powders [34, 35]:

i. Rotating cylinder method

ii. Oscillating method

iii. Inclined plane test

i) Rotating cylinder method

These viscometers consist of two concentric cylinders (Figure 11) the outer cylinder is usually a crucible and the inner cylinder (bob) is in movement. When a cylinder is rotated, it provides a velocity gradient and the torque developed is measured at different temperatures. There are two methods, (i) the rotating crucible method (RCR), in which the outer cylinder is rotated and (ii) the rotating cylinder method (RCyl) where the inner cylinder is rotated. Generally, all commercial instruments are of the latter type because of the simplicity of its construction. This method is the most widely used for this kind of materials.

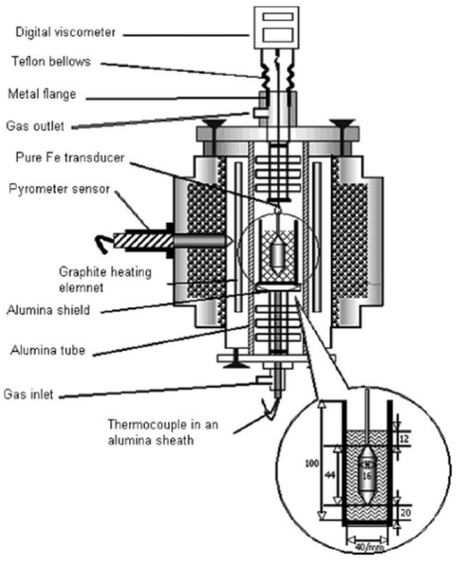

Figure 11. Rotating cylinder method used for measuring the viscosity of mould powders [36].

ii) Oscillating methods

The oscillating plate method is a relatively new method in which, subjected to a linear oscillating plate is submerged in the melt. As a result, there is a retarding force proportional to the viscosity of the fluid. When establishing a steady state, it records the amplitude of oscillation in air (φ_A) and in the melt (φ). This viscosity is derived from Eq. 16, where N is a constant, and$\rho$the density of the melt and G the constant load cell determined in calibration experiments.

$$\eta\rho = G\left[\frac{\varphi_A}{\varphi} - 1\right]^N \tag{16}$$

iii) Inclined plane test

This simple test has been used by some laboratories to estimate viscosities of molten fluxes. A mass of 10 g of powder is placed in a graphite crucible and then is melted at a specific temperature (T). The melted flux is maintained at that temperature for 15 min in order to achieve homogeneity. Then, the melt is fast cooled (quenched), pouring it onto an inclined plane. The length (L) of the ribbon is measured to have an estimation of the mould powder fluidity. In this case, the inverse of the length (1/L) is proportional to the viscosity of material at temperature T. Experimental trials in our laboratory indicated good reproducibility of results and very good relationship between ribbon lengths (L) and (1/η) for viscosities > 1 Poise (see Figure 12).

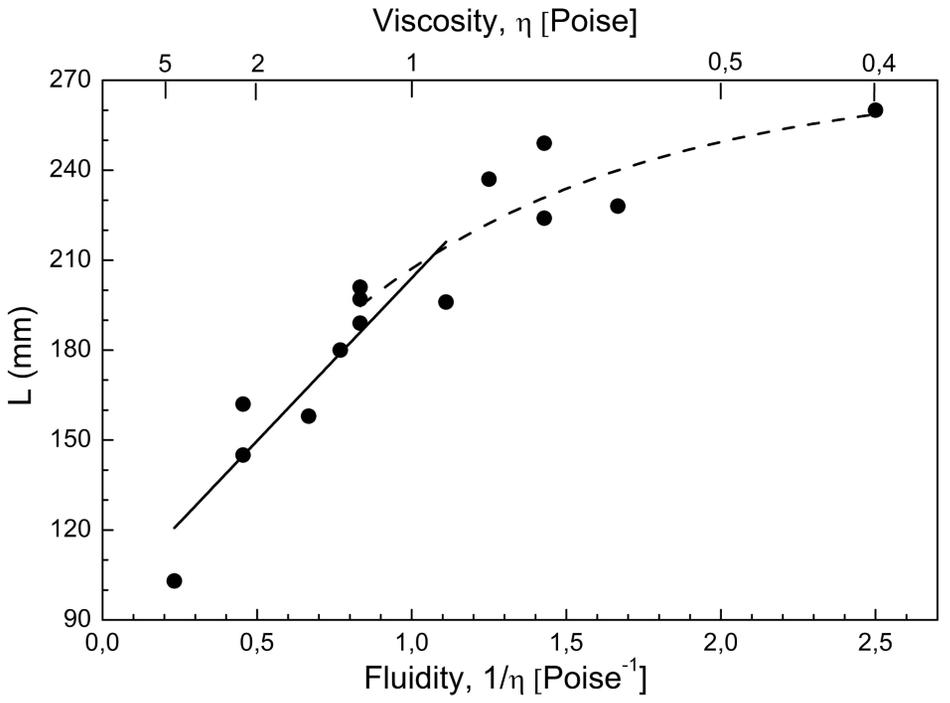

Figure 12. Slag ribbon length (L) as a function of fluidity (1/η).

5.4. Critical temperatures

The most widely used test to determine the melting range of a mould powder is the "high temperature microscopy test" (DIN 51730). The sample is pressed into a cylinder and placed in a furnace which continuously monitors the rate of heating and the changes in the sample shape. There are three critical temperatures determined by the cylinder morphology corresponding to the points of "softening", "hemisphere" and "fluidity" (see Figure 13). During the test of a commercial powder, the computer continuously analyzes variations in the shape of the sample and displays the resulting value of the critical temperatures.

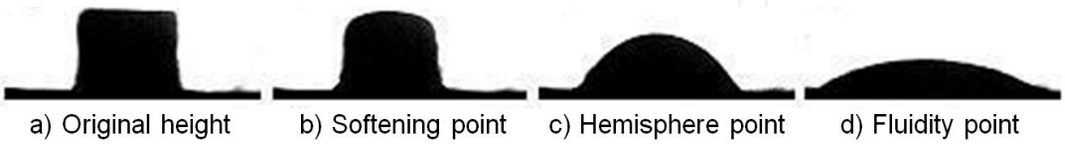

Figure 13. Image sequence showing critical temperatures of a commercial mould powder.

Another technique to determine the critical temperatures of the powders is by analyzing the ash fusibility. The test consists in prepare cones with the test material -mixed with a binder- and place them in a sample holder which is then inserted into the analyzer. Subsequently, the cones are heated to maintain a constant speed. Simultaneously, one sensor monitors the variation of the profile of the cones with temperature. At the end of the trial, the results are presented in form of four characteristic temperatures which are defined according to the morphology adopted by the cone: IT: initial temperature, ST: softening temperature, HT: hemispherical temperature, and FT: fluidity temperature.

6. Recent development in fluorine free mould fluxes

6.1. The fluoride evaporation problem associated with mould fluxes

As previously mentioned, many of the traditional mould fluxes used in continuous casting contain 4 to 10 wt % of CaF_2 in order to adjust their behaviuor according to the requirements of different steel grades casting process. At operation temperatures, harmful gas emissions (SiF_4, NaF) are produced and in many cases the gases in contact with water produce HF. These products can cause health problems to workers, affect the environment and they may cause damage to infrastructure of the plant (for example, to cooling system of the mould). Another aspect to consider is that losses of fluorides compounds also affect the chemical composition of the slag and may cause some changes in their behaviuor. For this reason, many researchers are searching substitute compounds for CaF_2 that can ensure the quality and behaviour of mould fluxes applied to slabs and long products casting [37-40].

Differential thermal analysis (DTA) and thermogravimetric (TG) data provide information about the kinetics of fluoride evaporation. By this technique, Persson et al. [38] report that the evaporation of these compounds occurs in the temperature range between 1400°C to 1600°C, in which the slags are one homogeneous liquid phase. CaF_2 is stable up to 900°C, so

any emission occurs at temperatures above it. According to the estimates obtained in our laboratory using software FactSage, the temperature of the gas release during the decomposition of pure CaF_2 (at normal conditions) begins at 1153°C. The principal reactions that may occur are showed in Eq. 17 (by contact of fluorite and SiO_2) and in Eq. 18 (by the combination of CaF_2 and water vapor of the slag):

$$2\,CaF_{2\,(slag)} + SiO_{2\,(slag)} \rightarrow SiF_{4\,(gas)} + 2\,CaO_{\,(slag)} \tag{17}$$

$$CaF_{2\,(slag)} + H_2O_{\,(slag)} \rightarrow 2\,HF_{\,(gas)} + CaO_{\,(slag)} \tag{18}$$

It is known that the reaction mechanism involves the diffusion of cations and anions in the liquid slag, reactions of ions promotes the formation of SiF_4 (gas) with the consequent generation of bubbles. Finally the bubbles migrate to the liquid-gas interface and SiF_4 escapes to the atmosphere. The results of the investigation of Persson et al [38] show that the loss of fluoride depends on the temperature and composition of the slag, increasing at higher contents of SiO_2.

6.2. Compounds replacing fluorine: effects of Na_2O, B_2O_3 and Li_2O oxides

It is important to consider the role of CaF_2 in mould fluxes. One major objective of incorporating such a compound is to decrease the viscosity, the melting temperature and to control cuspidine precipitation during cooling. The latter effect is especially important in the processing of slabs where heat extraction control has a high incidence on the surface quality of the product.

In this chapter, the physical properties of mould fluxes containing fluorine in their composition have been developed. A contribution through a comparative study of fluxes with and without fluoride compounds to evaluate the effect of some oxides or compounds which can be used as substitutes of F is presented.

The main oxides considered as potential substitutes for CaF_2 are: Na_2O, Li_2O, B_2O_3 [37, 40, 41]. Several researchers studied the effects of these compounds on the viscosity and the initial temperature of crystallization T_{br}. The effect of CaF_2 on the increase of percentage of crystallinity is largely known. However, some researchers suggest that MgO and B_2O_3 can act in opposite manner [37]. For a better understanding of the effects that the new possible oxides additions can have on the behaviour of mould fluxes, a comparison of the obtained results on the behaviour of fluxes with and without CaF_2 in relation with viscosity, fluidity and crystallinity, is detailed.

In order to determine the effect on: viscosity, fluidity and melting behaviour of the mentioned oxides, different samples of fluxes were prepared in the laboratory for experimental tests: A (10% F), B (6% B_2O_3 and 4% Li_2O), C (10% B_2O_3) and D (6% B_2O_3), which simulate the behaviuor of one commercial mould flux identified as PC that contains 10% F. Powder PC is commonly applied in the slab casting. In Table 2, the chemical composition of the samples is presented.

http://dx.doi.org/10.5772/50874

Compound	A (10% F)	B (6% B_2O_3 + 4% Li_2O)	C (10% B_2O_3)	D (6% B_2O_3)	PC (10% F)
SiO_2	37.1	33.2	36.6	34.6	36.3
Al_2O_3	5.4	4.7	5.1	5	5.1
B_2O_3	-	5.8	9.8	5.8	-
CaO	30.6	28.6	31.2	29.6	30.9
Na_2O	12.6	18.6	12.3	19.6	12.7
K_2O	0.1	0.1	0.1	0.1	0.7
MgO	1.3	1.4	1.3	1.4	2.1
F	9.5	-	-	-	10.5
Li_2O	-	3.9	-	-	-
MnO	-	-	-	-	0.1
Fe_2O_3	3.4	3.7	3.6	3.9	1.6
IB	0.82	0.86	0.85	0.86	0.85

Table 2. Chemical composition (in wt %)of the samples with and without CaF_2.

i) Viscosity

The importance of ensuring good lubrication to avoid sticking problems has been previously mentioned. It is known that this leads to require adequate viscosity of the mould flux during operation. For this reason, we analyze the comparative results obtained using the Riboud model to estimate viscosity values and their correlation with temperature (Figure 14).

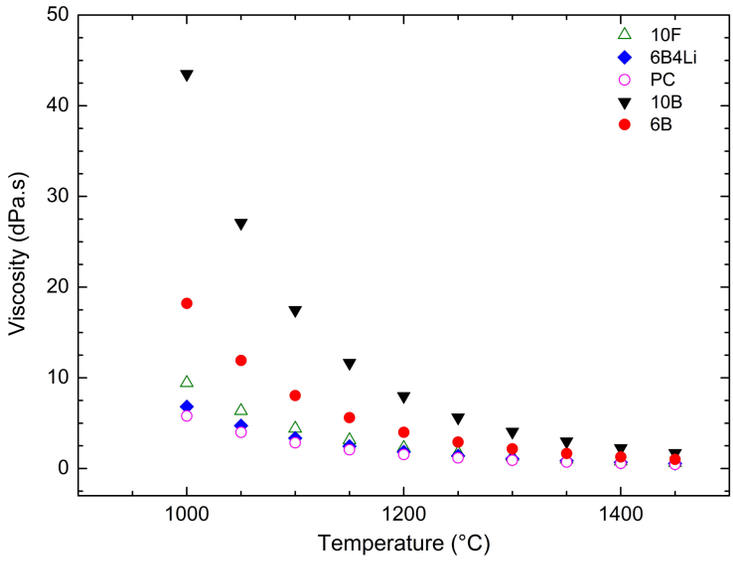

Figure 14. Correlation between viscosity and temperature of samples A, B, C, D and PC.

As it is observed the viscosities of the samples with (6% and 10% de B_2O_3) are the highest. Sample B that has 6% of the oxide is closest to the behaviour of commercial flux PC. It is noticeable that the addition of 4% Li_2O in sample B together with 6% B_2O_3, adjusts more precisely the viscosity behaviour with respect to PC flux. Higher contents than 6% of Li_2O cause a drastic decrease of viscosity and fluidity.

This suggests that the oxides considered in this study allow us to manipulate and adjust the viscosity of the mould fluxes to the required values for the processing of medium and low carbon steels. Furthermore, it is also possible to think in compensating a decrease of CaF_2 with a Na_2O increment in order to adjust the viscosity. In all samples, basicity values are around 0.85 such as PC.

The fluidity information obtained by the inclined plane test developed by Mills through the length of the layer (Lc) is consistent with the viscosity results reported in this chapter (Figure 15). The highest content of Na_2O in sample D, permits to justify the lowest fluidity obtained. Tandon et al. [42] studied the influence of high contents of Na_2O on the type of B-O bonds. The low oxide content promotes planar bonds and constitutes BO_3 but higher contents form stronger and tetrahedral bonds of BO_4.

As it is visualized, sample B (6% B_2O_3 and 4% Li_2O) is the one which presents a flow behaviour closer to the PC of reference. Samples with contents of 6% and 10% of B_2O_3 show a low fluidity because of their higher viscosity.

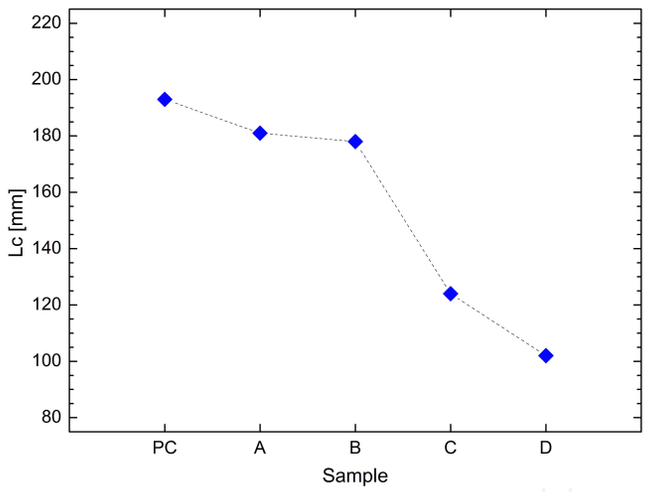

Figure 15. Fluidity behaviour of samples A, B, C, D and PC obtained by inclined plane test.

ii) Melting behaviour

The effect of the studied oxides on the melting behaviour of mould fluxes was also determined. In this case microscopy tests at high temperature (HSM) are carried out on all samples to determine the softening temperature (T_s), hemisphere temperature (T_h) and fluidity temperature (T_f). Figure 16 shows the results of the comparison between all the samples. Sample B (6% B_2O_3 and 4% Li_2O), is the one which presents the lowest critical temperatures.

http://dx.doi.org/10.5772/50874

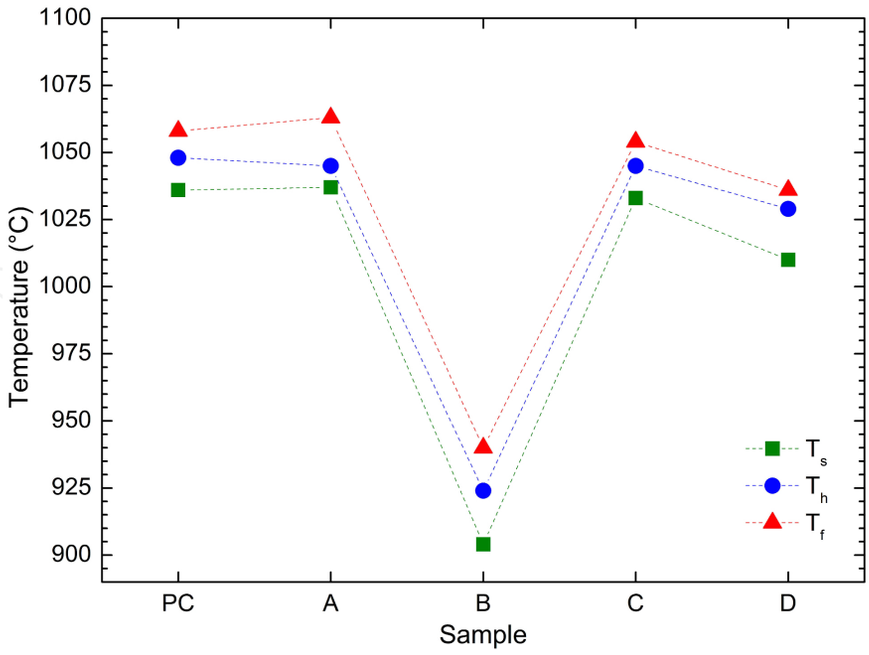

Figure 16. Melting behaviour of the samples PC, A, B, C and D.

Similar studies have been performed on mould fluxes applied in the processing of long products. In this application, mould fluxes are characterized by higher viscosities (2 to 3 Poise).

iii) Crystallization tendency

The heat extraction in the mould can be controlled by the crystalline proportion generated in the film of mould flux during the cooling stage. For this reason it is relevant to know the temperature at which the crystallization process begins (break temperature, T_{br}). Also, it is necessary to increase the knowledge of the crystallization mechanisms and tendency of mould fluxes at interest conditions.

The break temperature of the samples revealed that sample B (with 6% B_2O_3 and 4% Li_2O) presents a T_{br} = 1071°C and sample D (with 6% B_2O_3) a T_{br} = 1066°C. Both present a good agreement with PC sample in which T_{br} = 1064°C.

In the case of mould fluxes that are applied to long products casting, it is difficult to identify a clear change to verify the beginning of crystallization process because they are characterized by a high viscosity and a vitreous slag generation (or a supercooled liquid).

To evaluate the crystallization mechanisms of the samples, they were melted at 1300°C and then cooled drastically. These samples were identified as quenched (AQ). Then some of them were heat treated at different temperatures between 600°C and 870°C. All the samples were prepared for the microscopy study by light and electron scanning microscopy. Also, parts of the samples were ground to be analyzed by X-Ray Diffraction (XRD) and DTA.

The XRD results in PC at different temperatures show the evolution of the structure from a vitreous state to a crystalline one. The AQ sample is completely glassy. Nevertheless, sam-

ples treated at from 600°C produce a pronounced crystallization. In Figure 17a it is possible to observe the evolution of the crystal phases between 600°C and 850°C. By DTA, it was possible to identify the crystallization peaks of cuspidine (3 $CaO.2SiO_2.CaF_2$) present at all temperatures from 610°C, nepheline ($Al_4Ca0\ K_{0.8}Na_2Si_40_{16}$) at 729°C and villiaumite (NaF) at 854°C (Figure 17b).

Samples B and D, with (6% B_2O_3 and 4% Li_2O) and (6% B_2O_3) respectively, present different temperatures of crystallization. Sample B starts the crystallization at 610°C and sample D at 670°C. In Figure 18a, it is possible to observe the crystallization peaks of samples B and D and also the evolution of the crystallization peaks determined by DTA curves. It is found that the main phase in both cases is combeite ($Na_2Ca_2Si_3O_9$). In sample D the combeite crystallization peak is at 670°C and in sample B is at 610°C. The lower temperature in the crystallization peak of sample B could be due to the presence of Li_2O.

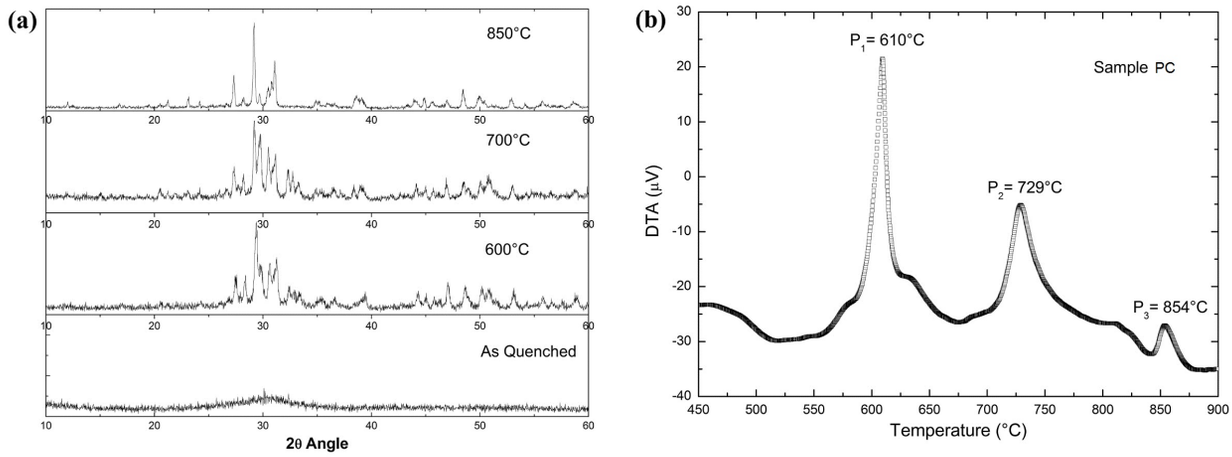

Figure 17. Crystallization evolution with temperature of sample PC: (a) XRD and (b) DTA.

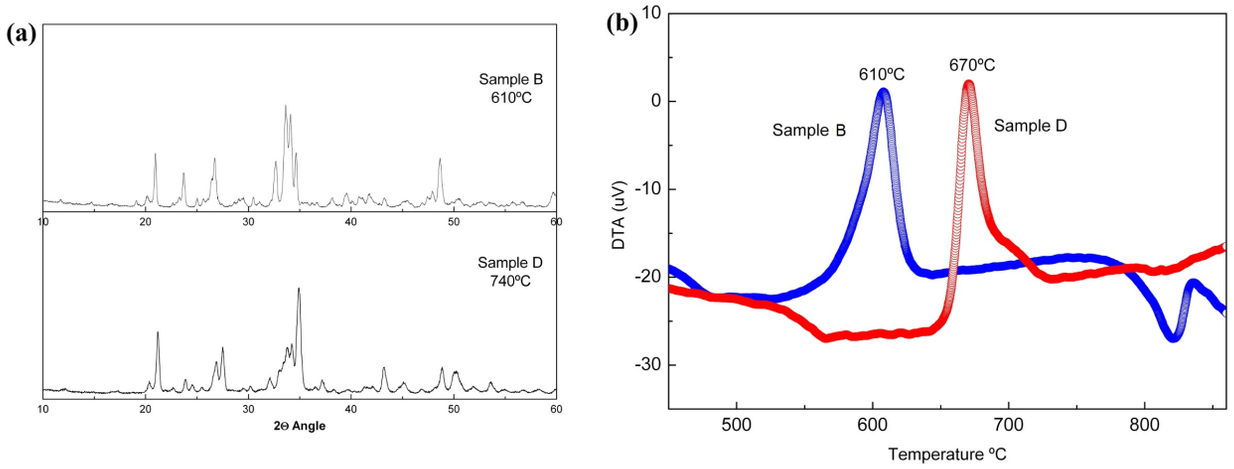

Figure 18. Crystallization evolution with temperature of samples B and D (a) XRD, (b) DTA.

http://dx.doi.org/10.5772/50874

Microscopy observations of all the samples permit to corroborate the information obtained by X ray diffraction and DTA curves. The crystallization mechanism begins at the surface of the samples where columnar crystals are developed. In samples PC and A crystals are constituted by cuspidine phase and in samples B and D by combeite phase. At higher temperatures (> 800°C), nuclei of irregular crystals appear in the inner part of the sample PC (Figure 19).

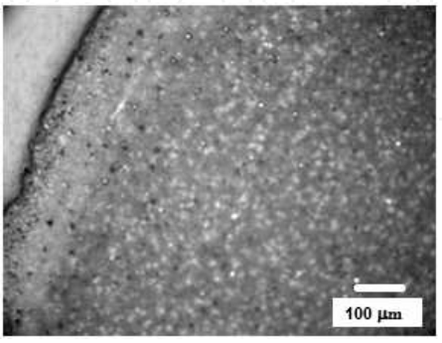

Figure 19. Morphology of sample PC at 850°C.

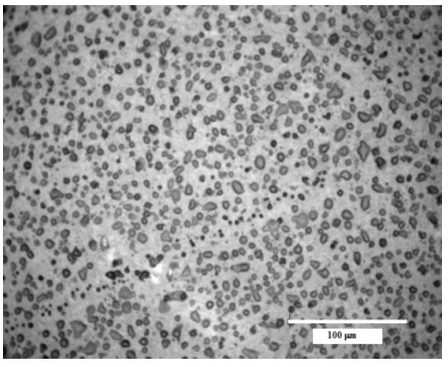

Figure 20. Liquid immiscibility phenomena observed at 610°C in sample B.

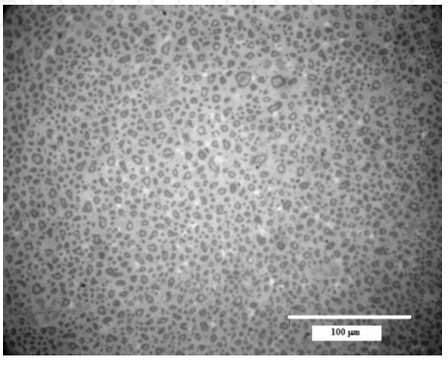

Figure 21. Liquid immiscibility phenomena observed at 680°C in sample D.

Samples B and D, present a liquid immiscibility phenomena (supercooled liquid effect), previous to the onset of the crystallization process (Figures 20, 21).

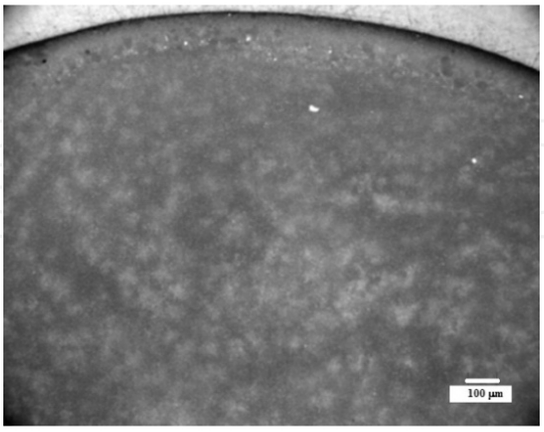

Figure 22. Morphology of sample B at 870°C.

In spite of liquid immiscibility and phase differences observed, the crystallization mechanism in the sample B at 870°C (Figure 22) is quite similar to sample PC. The presence of immiscible liquids phenomenon can be controlled by the degree of supercooling promoting a more homogeneous crystal nucleation.

Acknowledgements

The authors acknowledge the financial support of the Universidad Tecnológica Nacional (Argentina) and Ternium Siderar SAIC to promote the research in steel continuous casting process.

Author details

Elena Brandaleze[1], Gustavo Di Gresia[2], Leandro Santini[1], Alejandro Martín[1] and Edgardo Benavidez[1*]

*Address all correspondence to: ebenavidez@frsn.utn.edu.ar

1 Department of Metallurgy & DEYTEMA, Facultad Regional San Nicolás - Universidad Tecnológica Nacional, Argentina

2 Ternium Siderar SAIC, Argentina

References

[1] Mills, K., & Fox, A. (2002). Metals, Slags, Glasses: High Temperature Properties & Phenomena. *Mould Fluxes, Mills Symposium, The Institute of Materials*, 121-132.

[2] Thomas, B. (2001). Modeling of the Continuous Casting of Steel- Past, Present and Future. *Electric Furnace Conf. Proc. ISS*, 59, 3-30.

[3] Shin, H., Kim, S., Thomas, B., Lee, G., Park, J., & Sengupta, J. (2006). Measurement and Prediction of Lubrication, Powder Consumption, and Oscillation Mark Profiles in Ultra-low Carbon Steel Slabs. *ISIJ Int.*, 11, 1635-1644.

[4] Meng, Y., & Thomas, B. (2003). Heat Transfer and Solidification Model of Continuous Slab Casting: CON1D. *Met. Mat. Trans. B*, (34B), 5, 685-705.

[5] Wolf, M. (2003). Chapter 22. In: The AISE Steel Foundation, editors. Stainless Steels pp. 1-47.

[6] Mills, K. (1993). The Influence of Structure on the Physico-chemical Properties of Slags. *ISIJ Int.*, 33, 148-155.

[7] Waseda, Y., & Toguri, J. (1998). The Structure and Properties of Oxide Melts. World Scientific Publishing, Singapore.

[8] Mills, K., Chapman, L., Fox, A., & Sridhar, S. (2001). Round Robin Program for Slag Viscosity Estimation. *Scand. J. Metallurgy*, 30, 396-404.

[9] Riboud, P., Roux, Y., Lucas, L., & Gaye, H. (1981). Improvement of Continuous Casting Powders. *Fachberichte Huttenpraxis Metallweiterverarbeitung*, 19, 859-869.

[10] Iida, T. (2000). Accurate Prediction of the Viscosities of Various Industrial Slags from Chemical Composition. *J. High Temperature Soc.*, 25, 93-102.

[11] Brandaleze, E., & Benavidez, E. (2010). Effect of Different Oxides on Physical Properties of Complex Silicate Systems. 95° Physics National Meeting. Malargüe, Argentina.

[12] Moynihan, C. (1993). Correlation between the Width of the Glass Transition Region and the Temperature Dependence of the Viscosity of High-Tg Glasses. *J. Am. Ceram. Soc.*, 76, 1081-1087.

[13] Eriksson, R., Hayashi, M., & Seetharaman, S. (2003). Thermal Diffusivity Measurements of Liquid Silicate Melts. *Int. J. Thermophysics*, 24, 785-797.

[14] Hayashi, M., Ishii, H., Susa, M., Fukuyama, H., & Nagata, K. (2001). Effect of Ionicity of Non-bridging Oxygen Ions on Thermal Conductivity of Molten Alkali Silicates. *Phys. Chem. Glasses*, 42, 6-11.

[15] Hanao, M., & Kawamoto, M. (2008). Flux Film in the Mould of High Speed Continuous Casting. *ISIJ Int.*, 48, 180-185.

[16] Brandaleze, E., Martín, A., Benavidez, E., Santini, L., & Di Gresia, G. (2008). Development of an Equipment for the Measurement of Thermal Conductivity in Mould Fluxes. *Proceedings of 39th International Steelmaking Seminar*, ABM. In CD.

[17] Ozawa, S., Susa, M., Goto, T., Endo, R., & Mills, K. (2006). Lattice and Radiation Conductivities for Mould Fluxes from the Perspective of Degree of Crystallinity. *ISIJ Int.*, 46, 413-419.

[18] Nakada, H., Susa, M., Seko, Y., Hayashi, M., & Nagata, K. (2008). Mechanism of Heat Transfer Reduction by Crystallization of Mould Flux for Continuous Casting. *ISIJ Int.*, 48, 446-453.

[19] Mills, K. (1986). ACS Symposium Series 301 Mineral Mater and ash in coal. In: Vorres KS, editors. Estimation of Physicochemical Properties of Coal Slags. *Am. Chem. Soc.*, 195-214.

[20] Nakamoto, M., Tanaka, T., Holappa, L., & Hämäläinen, M. (2007). Surface Tension Evaluation of Molten Silicates Containing Surface-active Components (B_2O_3, CaF_2 or Na_2O). *ISIJ Int.*, 47, 211-216.

[21] Sridhar, S., Mills, K., Afrange, O., Lörz, H., & Carli, R. (2000). Break Temperatures of Mould Fluxes and Their Relevance to Continuous Casting. *Ironmaking and Steelmaking*, 27, 238-242.

[22] Brandaleze, E., Santini, L., Gorosurreta, C., & Martín, A. (2007). Influence of Carbonaceous Particles on the Melting Behaviour of Mould Fluxes at High Temperature. *Proceedings of 16th Steelmaking Conference IAS, Argentina*, 363-371.

[23] Wei, E., Yang, Y., Feng, C., Sommerville, I., & McLean, A. (2006). Effect of Carbon Properties on Melting Behavior of Mould Fluxes for Continuous Casting of Steel. *J. Iron Steel Res.*, 13, 22-26.

[24] Benavidez, E., Santini, L., & Brandaleze, E. (2011). Decomposition Kinetic of Carbonaceous Materials Used in a Mould Flux Design. *J. Therm. Anal Cal.*, 103, 485-493.

[25] Persson, M., Matsushita, T., Zhang, J., & Seetharaman, S. (2007). Estimation of Molar Volumes of some Binary Slags from Enthalpies of Mixing. *Steel Res. Int.*, 78, 102-108.

[26] Schwerdtfeger, K. (1983). Heat Transfer Through Layers of Casting Fluxes. *Ironmaking and Steelmaking*, 10, 24-30.

[27] Mikrovas, A., Agyropoulos, A., & Sommerville, I. (1991). Measurements of the Effective Thermal Conductivity of Liquid Slags and Mould Powders. *Ironmaking and Steelmaking*, 18(3), 169-181.

[28] Jenkins, M. (1995). Characterization and Modification of the Heat Transfer Performance of Mould Powders. *Steelmaking Conference Proceedings, ISS*, 78(3), 667-669.

[29] Yamauchi, A., & Sorimachi, K. (1993). Heat Transfer between Mould and Strand through Mould flux Film in Continuous Casting of Steel. *ISIJ Int.*, 33(1), 140-147.

[30] Mills, K. (1994). Thermal Properties of Slag Films Taken From Continuous Casting Mould. *Iron and Steelmaking*, 21(4), 279-286.

[31] Holzhauser, J. (1999). Laboratory Study of Heat Transfer through Thin Layers of Casting Steel. *Steel Research*, 70(10), 430-436.

[32] Stone, D., & Thomas, B. (1999). Measurement and Modeling of Heat Transfer Across Interfacial Mould Flux Layer. *Canadian Metallurgical Quarterly*, 38(5), 363-375.

[33] Martín, A., Brandaleze, E., Santini, L., & Benavidez, E. (2011). Study on a Mould Powder Layer Extracted During the Continuous Casting Process. *Proceedings of 18th Steelmaking Conference IAS*, 73-83.

[34] Mills, K. (1995). Viscosities of Molten Slags. In: Verein Deutscher Eisenhüttenleute editors. Slag Atlas, Second Edition. Mills: Verlag Stahleisen GmbH, pp. 349-352.

[35] Brooks, R., Dinsdale, A., & Quested, P. (2005). The Measurement of Viscosity of Alloys- a Review of Methods, Data and Models. *Meas. Sci. Techol.*, 16, 354-362.

[36] Persson, M., Görnerup, M., & Seetharaman, S. (2007). Viscosity Measurements of Some Mould Fluxes Slags. *ISIJ Int.*, 47(10), 1533-1540.

[37] Fox, A., Mills, K., Lever, D., Bezerra, C., Valadares, C., & Unamuno, I. (2005). Development of Fluoride-free Fluxes for Billet Casting. *ISIJ Int.*, 45(7), 1051-1058.

[38] Persson, M., Seetharaman, S., & Seetharaman, S. (2007). Kinetic Studies of Fluoride Evaporation from Slags. *ISIJ Int.*, 47(12), 1711-1717.

[39] Li, G., Wang, H., Dai, Q., Zhao, Y., & Li, J. (2007). Physical Properties and Regulating Mechanism of Fluoride-free and Harmless B_2O_3 Containing Mould Flux. *Journal of Iron and Steel Research International*, 14(1), 25-28.

[40] Brandaleze, E., Benavídez, E., Peirani, V., Santini, L., & Gorosurreta, C. (2010). Impact of Free Fluor Fluxes on Nozzle Wear Mechanisms. *Advances Science and Technology*, 70, 205-210.

[41] Kim, G., & Sohn, I. (2012). Influence of Li_2O on the Viscous Behaviour of CaO-Al_2O_3-12 Mass% Na_2O-12 Mass % CaF_2 Based Slags. *ISIJ Int.*, 52(1), 68-73.

[42] Tandon, S., Agrawal, R., & Kapoor, M. (1994). Viscosity of Molten Na_2O-B_2O_3 Slags. *J. Am. Ceram. Soc.*, 77(4), 1032-1036.

IntechOpen